Accurate Time-Domain Fault Location Method on Practically Transposed Transmission Lines

Dayou Lu[1], *Student Member, IEEE*, Yu Liu[1,*], *Member, IEEE*, Binglin Wang[1], *Student Member, IEEE*, Lihui Yi[1], *Student Member, IEEE*, and Xiaodong Zheng[2], *Senior Member, IEEE*
1. School of Information Science and Technology, ShanghaiTech University, Shanghai, China, 201210
2. Department of Electrical Power Engineering, Shanghai Jiao Tong University, Shanghai, China, 200240
*Email: liuyu.shanghaitech@gmail.com

***Abstract*—Accurate fault location reduces time searching for the fault and the power system operational cost. This paper proposes a time domain fault location method for practically transposed transmission lines. Unlike the ideally transposed lines which assumed to be transposed infinite number of times, the transposed lines in practice is transposed for very limited times. First, the practically transposed line is modeled as a non-homogenous line, consisting of several untransposed line sections. Afterwards, the eigenvalue decomposition is applied to decouple each untransposed line section and the Bergeron model is applied to solve the voltage distribution through the entire non-homogeneous line. Finally, the voltage method is applied to locate the fault using the calculated voltage distribution. Extensive numerical experiments verify that the proposed fault location method presents higher fault location accuracy compared to the existing method that simply assumes ideal transposition for practically transposed transmission lines.**

Key words—fault location, practically transposed transmission line, time domain, Bergeron model.

I. INTRODUCTION

ACCURATE fault location reduces the time searching for the fault, the power outage time, and the system operational cost. The alternating current (AC) transmission lines are usually constructed with the options of untransposed or transposed lines. For untransposed lines, the physical arrangement of each phase conductor remains the same for the entire span of the line. Due to the geometrical asymmetry of the tower structure, the voltages and currents within the untransposed lines are not symmetrical, which may cause three phase unbalancing issues. Therefore, line transposition is widely adopted for three phase balancing especially for the high voltage long line, by exchanging the position of phase conductors such that each phase occupies all positions of a particular line configuration [1]. For the faults occur on the transmission lines, varies fault location methods are proposed for both the untransposed lines and the transposed lines. The fault location methods can be mainly classified into measurement based methods and model based methods.

The most widely adopted measurement based methods are the traveling wave based methods [2]-[4]. Traveling wave based methods locate the fault by determining the arrival time of wavefronts. The accuracy of the traveling wave based methods dependents on the accurately detection of the wavefront, which requires a high sampling rate and may be challenging during faults with zero fault angle. In addition, to minimize the influence of the mutual coupling between phases, constant transformations (eg. Clarke transformation) are typically applied in traveling wave based methods. For untransposed lines, the Clarke transformation cannot perfectly decouple the voltages and currents of three phases, which may introduce fault location errors.

The model based methods locate the fault via the analysis of the relationship between the fault location and available measurements using certain transmission line models. Model based methods further include phasor domain methods and time domain methods. The most widely adopted phasor domain methods are the impedance based methods [1]. The Clarke transformation is also typically applied to decouple the system. Other phasor domain methods are also proposed for both transposed lines [5], [6] and untransposed lines [6]-[8]. The main challenge of phasor domain methods is the accurate calculation of phasors, especially when the available data window during the fault is short due to high speed tripping of the protective relays. Consequently, the time domain model based methods are proposed.

The time domain model based methods can be further classified into methods of solving equations and voltage methods. The methods of solving equations formulate equations where the fault location is introduced as an unknown variable, using either transposed [9] or untransposed [10], [11] line model. The solution of the equation shows the fault location. However, to formulate these equations, the lumped parameter models are usually applied. The voltage methods locate the fault by calculation of the voltage distribution. The extremum of the voltage distribution shows the fault location. The distributed parameter model can be applied to solve the voltage distribution for both transposed and untransposed lines [12], [13].

For model based methods for transposed lines, besides the accuracy of the model applied in fault location algorithm, there is another very important factor that may generate fault location errors. For transposed lines, the aforementioned fault location methods typically treat the transmission line as a homogeneous ideally transposed line, with the assumption that the line is perfectly transposed for infinite number of times to ensure absolute symmetry. However in practice, the transmission line is transposed for very limited times. A widely adopted practical transposition strategy is to rotate phase conductors every one-third of the total line length [1], dividing the overall transmission line into three homogeneous untransposed sections with the same section length. In fact, the ideally transposed line model (ITLM) and the practically transposed line model (PTLM) can be equivalent if one only focus on relationships of voltages and currents at line terminals during normal operation. However, for the fault location problem, since the fault usually occurs inside the line instead of at terminals, the assumption of ITLM will generate fault location errors. **For fault location on transposed lines, most existing fault location methods assume ideal transposition of the line, resulting in fault location errors in practical transposed lines. This issue has only been discussed by very few literatures** [14], [15] **and has not been fully investigated.** Reference [14] proposed a fault location method using PTLM in phasor domain. When the available data window during the fault is short, the fault location accuracy could be compromised. Reference [15] proposed a time domain method of solving equation using PTLM with the lumped R-L parameters. For long lines, assuming lumped parameters and neglecting distributed shunt capacitances will generate fault location errors.

In this paper, a time domain voltage method fault location is

This work is sponsored by National Nature Science Foundation of China (No. 51807119). The support is greatly appreciated.

proposed using PTLM with distributed parameters. First, the practically transposed line is modeled as a non-homogeneous line with several untransposed line sections. Afterwards, the eigenvalue decomposition is applied to decouple each untransposed line section. The Bergeron model, which considers the distributed line inductances/capacitances as well as the lumped line resistances, is applied to solve the voltage distribution for entire transmission line. Finally, the voltage method is applied to locate the fault with the calculated voltage distribution. Extensive numerical experiments in a 300 km three phase practically transposed line system verify that, the proposed fault location method using PTLM presents higher fault location accuracy compared to the existing method using ITLM.

The rest of the paper is organized as follows. Section II shows details of the PTLM and derives the calculation of the voltage distribution. Section III introduces the fault location algorithm. Section IV demonstrates the numerical experimental results of the fault location. Section V draws a conclusion.

II. Modeling of Practically Transposed Lines

The PTLM is shown in Figure 1. The entire transmission line is separated into three sections *k*1-*k*2, *k*2-*k*3 and *k*3-*k*4 (each section is an untransposed line), with the section length of l_1, l_2, l_3 and the phase sequence of *ABC*, *CAB* and *BCA*. The transmission line is rotated at the terminal of each line section as shown in the figure. $\boldsymbol{R}$, $\boldsymbol{L}$ and $\boldsymbol{C}$ are the resistance, inductance and capacitance matrices per unit length of each untransposed transmission line (the line conductance is ignored). Note that for practically transposed lines, since the tower structure of each untransposed line section is the same, the three sections share the same $\boldsymbol{R}$, $\boldsymbol{L}$ and $\boldsymbol{C}$ parameter matrices.

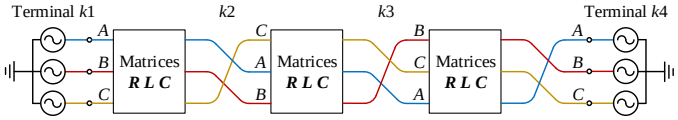

Figure. 1. Practically transposed transmission line model

For the voltage method fault location, the calculation of the voltage distribution of entire practically transposed line from one terminal requires proper rotation of phase voltages and currents at each terminal of line sections. These rotations increase the complexity of the model. Next, the solution of the voltage distribution for practically transposed transmission line is derived. First, the methodology of the transformation of the practically transposed line into one non-homogeneous line is introduced. Second, the eigenvalue decomposition is applied to decouple each untransposed line section. Third, the Bergeron model is applied to solve the voltage distribution.

A. Equivalent Non-homogeneous Line Model

The construction of the equivalent non-homogeneous line model is to present the mathematical equation to describe the physical laws of the practically transposed transmission line. The physical laws of three line sections can be describes as,

$$\begin{cases} \partial \boldsymbol{u}(x,t)/\partial x+\boldsymbol{L}\partial \boldsymbol{i}(x,t)/\partial t+\boldsymbol{R}\boldsymbol{i}(x,t)=\boldsymbol{0} \\ \partial \boldsymbol{i}(x,t)/\partial x+\boldsymbol{C}\partial \boldsymbol{u}(x,t)/\partial t=\boldsymbol{0} \end{cases} ,x\in[0,l_1]$$
$$\begin{cases} \boldsymbol{T}_R\partial \boldsymbol{u}(x,t)/\partial x+\boldsymbol{L}\boldsymbol{T}_R\partial \boldsymbol{i}(x,t)/\partial t+\boldsymbol{R}\boldsymbol{T}_R\boldsymbol{i}(x,t)=\boldsymbol{0} \\ \boldsymbol{T}_R\partial \boldsymbol{i}(x,t)/\partial x+\boldsymbol{C}\boldsymbol{T}_R\partial \boldsymbol{u}(x,t)/\partial t=\boldsymbol{0} \end{cases} ,x\in[l_1,l_1+l_2] \quad (1)$$
$$\begin{cases} \boldsymbol{T}_R{}^2\partial \boldsymbol{u}(x,t)/\partial x+\boldsymbol{L}\boldsymbol{T}_R{}^2\partial \boldsymbol{i}(x,t)/\partial t+\boldsymbol{R}\boldsymbol{T}_R{}^2\boldsymbol{i}(x,t)=\boldsymbol{0} \\ \boldsymbol{T}_R{}^2\partial \boldsymbol{i}(x,t)/\partial x+\boldsymbol{C}\boldsymbol{T}_R{}^2\partial \boldsymbol{u}(x,t)/\partial t=\boldsymbol{0} \end{cases} ,x\in[l_1+l_2,l_1+l_2+l_3]$$

where x is the distance from the local terminal *k*1 of the line, $\boldsymbol{0}$ is the 3-dimensional zero vector, $\boldsymbol{u}(x,t)=\left[u_A(x,t)\ u_B(x,t)\ u_C(x,t)\right]^{\mathrm{T}}$, $\boldsymbol{i}(x,t)=\left[i_A(x,t)\ i_B(x,t)\ i_C(x,t)\right]^{\mathrm{T}}$, $u_j(x,t)$ and $i_j(x,t)$ $(j=A,B,C)$ are voltages and currents of phase j, the current direction is consistent with the positive direction of x. $\boldsymbol{T}_R$ is the rotation matrix and is defined as,

$$\boldsymbol{T}_R=\begin{bmatrix} 0 & 1 & 0 \\ 0 & 0 & 1 \\ 1 & 0 & 0 \end{bmatrix} \quad (2)$$

From (1) and (2), the physical laws for entire practically transposed transmission line can be described as,

$$\begin{cases} \partial \boldsymbol{u}(x,t)/\partial x+\boldsymbol{L}_1\partial \boldsymbol{i}(x,t)/\partial t+\boldsymbol{R}_1\boldsymbol{i}(x,t)=\boldsymbol{0} \\ \partial \boldsymbol{i}(x,t)/\partial x+\boldsymbol{C}_1\partial \boldsymbol{u}(x,t)/\partial t=\boldsymbol{0} \end{cases} ,x\in[0,l_1]$$
$$\begin{cases} \partial \boldsymbol{u}(x,t)/\partial x+\boldsymbol{L}_2\partial \boldsymbol{i}(x,t)/\partial t+\boldsymbol{R}_2\boldsymbol{i}(x,t)=\boldsymbol{0} \\ \partial \boldsymbol{i}(x,t)/\partial x+\boldsymbol{C}_2\partial \boldsymbol{u}(x,t)/\partial t=\boldsymbol{0} \end{cases} ,x\in[l_1,l_1+l_2] \quad (3)$$
$$\begin{cases} \partial \boldsymbol{u}(x,t)/\partial x+\boldsymbol{L}_3\partial \boldsymbol{i}(x,t)/\partial t+\boldsymbol{R}_3\boldsymbol{i}(x,t)=\boldsymbol{0} \\ \partial \boldsymbol{i}(x,t)/\partial x+\boldsymbol{C}_3\partial \boldsymbol{u}(x,t)/\partial t=\boldsymbol{0} \end{cases} ,x\in[l_1+l_2,l_1+l_2+l_3]$$

where $\boldsymbol{P}_1=\boldsymbol{P}$, $\boldsymbol{P}_2=\boldsymbol{T}_R{}^{-1}\boldsymbol{P}_1\boldsymbol{T}_R$, $\boldsymbol{P}_3=\boldsymbol{T}_R{}^{-1}\boldsymbol{P}_2\boldsymbol{T}_R$ and $\boldsymbol{P}$ corresponds to the parameter matrices $\boldsymbol{R}$, $\boldsymbol{L}$ and $\boldsymbol{C}$.

Therefore, according to (3), the equivalent three-section non-homogeneous line model is shown in Figure 2.

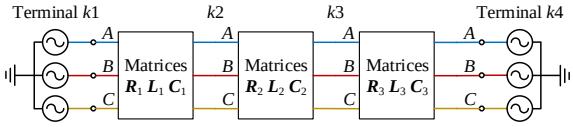

Figure. 2. Equivalent transmission line model

B. Eigenvalue Decomposition

The solution of the non-homogeneous line model (3) gives the voltage distribution of entire transmission line. For the solution of each untransposed section, consider a general untransposed line model (with parameter matrices of $\boldsymbol{R}$, $\boldsymbol{L}$, $\boldsymbol{C}$, line length of l, line terminals denoted as k and m) with following partial differential equation,

$$\begin{cases} \partial \boldsymbol{u}(x,t)/\partial x+\boldsymbol{L}\cdot\partial \boldsymbol{i}(x,t)/\partial t+\boldsymbol{R}\cdot\boldsymbol{i}(x,t)=\boldsymbol{0} \\ \partial \boldsymbol{i}(x,t)/\partial x+\boldsymbol{C}\cdot\partial \boldsymbol{u}(x,t)/\partial t=\boldsymbol{0} \end{cases} \quad (4)$$

Equation (4) can be decoupled via eigenvalue decomposition [16]. After applying the eigenvalue decomposition to matrix $\boldsymbol{LC}$, $\boldsymbol{T}_u$ is the eigenmatrix of $\boldsymbol{LC}$, and $\boldsymbol{\Lambda}_{LC}$ is a diagonal matrix where the diagonal elements correspond to the eigenvalues of $\boldsymbol{LC}$. These matrices satisfy $\boldsymbol{T}_u{}^{-1}\boldsymbol{L}\boldsymbol{C}\boldsymbol{T}_u=\boldsymbol{\Lambda}_{LC}$. The inductance matrix $\boldsymbol{L}$ and capacitance matrix $\boldsymbol{C}$ can be diagonalized as $\boldsymbol{\Lambda}_L=\boldsymbol{T}_u{}^{-1}\boldsymbol{L}\boldsymbol{T}_i$ and $\boldsymbol{\Lambda}_C=\boldsymbol{T}_i{}^{-1}\boldsymbol{C}\boldsymbol{T}_u$, where $\boldsymbol{T}_i=\left(\boldsymbol{T}_u{}^{-1}\right)^T$. For resistance matrix, ignore the off-diagonal elements of matrix $\boldsymbol{T}_u{}^{-1}\boldsymbol{R}\boldsymbol{T}_i$ as $\boldsymbol{\Lambda}_R$. Define the mode voltage as $\boldsymbol{u}_m(x,t)=\boldsymbol{T}_u{}^{-1}\boldsymbol{u}(x,t)$ and the mode current as $\boldsymbol{i}_m(x,t)=\boldsymbol{T}_i{}^{-1}\boldsymbol{i}(x,t)$, equation (4) can be decoupled into three modes, where for each mode j (j = 1, 2, 3),

$$\begin{cases} \partial u_j(x,t)/\partial x+L_j\partial i_j(x,t)/\partial t+R_j i_j(x,t)=0 \\ \partial i_j(x,t)/\partial x+C_j\partial u_j(x,t)/\partial t=0 \end{cases} \quad (5)$$

where u_j and i_j are the j^{th} elements of vectors $\boldsymbol{u}_m$ and $\boldsymbol{i}_m$, respectively; L_j, R_j and C_j are the j^{th} diagonal elements of the matrices $\boldsymbol{\Lambda}_L$, $\boldsymbol{\Lambda}_R$ and $\boldsymbol{\Lambda}_C$, respectively.

C. Solution of Voltage Distribution with Bergeron Model

The Bergeron model describes the relationship between the voltages and currents at terminals of a transmission line [17]. It

first ignores the terms with R_j in (5) to obtain the analytical solution for a lossless transmission line. Afterwards, the effect of resistance is considered by adding lumped resistors at the terminals and the mid-point of the line. The Bergeron model gives the solution of (5) as,

$$\begin{aligned} i_{kj}(t) &= 1/Z_j \cdot u_{kj}(t) - (1+h_j)/2 \cdot \left[1/Z_j \cdot u_{mj}(t-\tau_j) \right. \\ &\left. + h_j i_{mj}(t-\tau_j)\right] - (1-h_j)/2 \cdot \left[1/Z_j \cdot u_{kj}(t-\tau_j) + h_j i_{kj}(t-\tau_j)\right] \\ i_{mj}(t) &= 1/Z_j \cdot u_{mj}(t) - (1+h_j)/2 \cdot \left[1/Z_j \cdot u_{kj}(t-\tau_j) \right. \\ &\left. + h_j i_{kj}(t-\tau_j)\right] - (1-h_j)/2 \cdot \left[1/Z_j \cdot u_{mj}(t-\tau_j) + h_j i_{mj}(t-\tau_j)\right] \end{aligned} \quad (6)$$

where $i_{kj}(t)$, $u_{kj}(t)$, $i_{mj}(t)$ and $u_{mj}(t)$ denote the currents and voltages at terminals k and m of the line: $i_{kj}(t) = i_j(0,t)$, $i_{mj}(t) = -i_j(l,t)$, $u_{kj}(t) = u_j(0,t)$ and $u_{mj}(t) = u_j(l,t)$, $h_j = \left(\sqrt{L_j/C_j} - lR_j/4\right) \Big/ \left(\sqrt{L_j/C_j} + lR_j/4\right)$, $Z_j = \sqrt{L_j/C_j} + lR_j/4$ and $\tau_j = l\sqrt{L_j C_j}$ is the wave traveling time of the entire line of mode j.

In purpose of solving the voltage distribution through the entire transmission line with the measurements at one terminal for voltage method, express the voltage at one terminal of the line with the voltage and current at another terminal,

$$\begin{aligned} u_{mj}(t) &= 2Z_j \Big/ (1+h_j)^2 \cdot \left[1/Z_j \cdot u_{kj}(t+\tau_j) - i_{kj}(t+\tau_j)\right] \\ &- \left[(1-h_j)/(1+h_j)\right]^2 \cdot u_{kj}(t) - 2h_j(1-h_j)/(1+h_j)^2 \cdot Z_j i_{kj}(t) \\ &+ 2h_j{}^2/(1+h_j)^2 \cdot Z_j \left[1/Z_j \cdot u_{kj}(t-\tau_j) + h_j \cdot i_{kj}(t-\tau_j)\right] \end{aligned} \quad (7)$$

The solution of the terminal current is,

$$\begin{aligned} -i_{mj}(t) &= -\left\{2/(1+h_j)^2 \cdot \left[1/Z_j \cdot u_{kj}(t+\tau_j) - i_{kj}(t+\tau_j)\right] \right. \\ &-2(1-h_j)/(1+h_j)^2 \cdot 1/Z_j \cdot u_{kj}(t) + (1-h_j)^2/(1+h_j)^2 \cdot i_{kj}(t) \\ &\left. -2h_j/(1+h_j)^2 \cdot \left[1/Z_j \cdot u_{kj}(t-\tau_j) + h_j \cdot i_{kj}(t-\tau_j)\right]\right\} \end{aligned} \quad (8)$$

In the equivalent transmission line model as shown in Figure 2, apply (7) to the untransposed section $k1$-$k2$ with the line length l varying between [0, l_1]. The mode voltage distribution $\boldsymbol{u}_m(x,t)$ is solved with the voltage and current measurements at line terminal $k1$. The phase voltage distribution is obtained as $\boldsymbol{u}(x,t) = \boldsymbol{T}_u \boldsymbol{u}_m(x,t)$. In addition, apply (7) and (8) with the line length equal to l_1, the phase voltages and currents at node $k2$ are solved. Next, consider the solved phase voltages and currents at node $k2$ as the new terminal measurements for line section $k2$-$k3$ and repeat above process. The voltage distribution on line section $k2$-$k3$ can also be solved (similarly for line section $k3$-$k4$). Note that for different line sections, the parameter matrices are different (corresponds to $\boldsymbol{P}_1$, $\boldsymbol{P}_2$ and $\boldsymbol{P}_3$). Therefore, the eigenvalue decomposition matrices in section II. B for each line section is also different. With above process, the voltage distribution along the entire practically transposed line is solved with voltage and current measurements at only one terminal $k1$. The solution with measurements at terminal $k4$ is similar. Then the voltage method can be applied to locate the fault.

III. Fault Location Algorithm

In this section, the voltage method fault location algorithm for practically transposed transmission line is proposed with the calculated voltage distributions from either terminal of the line. The essence of the voltage method is that, the voltage distribution solved from one terminal is only correct before the fault location. For the two voltage distribution curves calculated from two terminals respectively, only the voltage at fault location is solved both correctly and identically. Therefore, the intersection of the two voltage distribution curves determines the fault location. To improve the accuracy of the fault location, the following optimization problem is formulated,

$$\min_x F(x) = \min_x \left(\sum_{t=\tau_{\text{sum}}}^{t_f - \tau_{\text{sum}}} \left| u^{(k1)}(x,t) - u^{(k4)}(x,t) \right| \right) \quad (9)$$

where $u^{(k1)}(x,t)$ and $u^{(k4)}(x,t)$ are the voltage distributions calculated from two terminals $k1$ and $k4$ respectively, $u^{(j)}(x,t)$ (j = $k1$, $k4$) is the line mode voltage, according to the fault type (eg. $u^{(j)}(x,t) = 2u_A{}^{(j)}(x,t) - u_B{}^{(j)}(x,t) - u_C{}^{(j)}(x,t)$ for phase A to G faults and three phase faults, $u^{(j)}(x,t) = u_B{}^{(j)}(x,t) - u_C{}^{(j)}(x,t)$ for phase B to C faults and phase BC to G faults). $[\tau_{\text{sum}}, t_f - \tau_{\text{sum}}]$ is the summation window in (9), with the available data window of $[0, t_f]$, τ_{sum} is the summation (of three section) of the maximum (of three mode) wave traveling time $\tau_{\max}^s$ (section number s = 1, 2, 3).

To reduce the computation complexity, a two-iteration fault location algorithm is adopted [13]. The first iteration calculates the approximate fault location with a relatively large distance interval. The second iteration calculates the accurate fault location with small distance interval, by recalculating the voltage distribution along the small segment of the line around the approximate fault location. The flow chart of the fault location algorithm is shown in Figure 3.

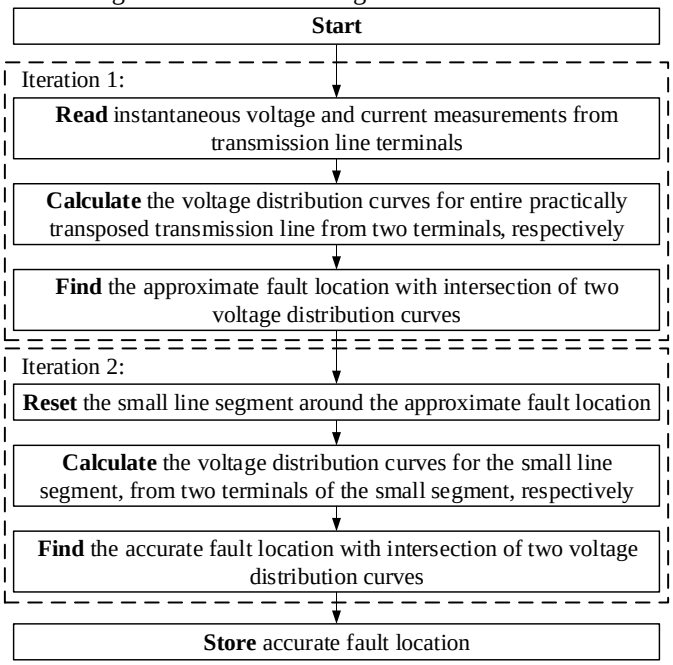

Figure. 3. Flow chart of the fault location algorithm

IV. Numerical Validation

The proposed fault location algorithm is numerically validated with a 300 km 500 kV three phase practically transposed AC transmission line. The test system is shown in Figure 1, with the tower structure shown in Figure 4. From

Figure 4, the line consists of three untransposed line sections, where the tower structure for each line section is geometrically asymmetrical (the parameters for phase A B and C are not exactly the same). The transmission line is rotated at the location of every 100 km. Note that in a real power system, the length of each section could be slightly different. Nevertheless, the proposed method still works in this situation since the method does not have assumption on the length of each untransposed section. Here the length of each section is selected to be identical, to exhibit a better comparison between PTLM and ITLM (same length ensures that from the terminal of the line a practically transposed line presents exactly the same as an ideally transposed line; the different section length results in larger modeling inconformity for ITLM). The test system is built in PSCAD/EMTDC with frequency dependent (phase) model. The phase angles of phase A voltage for sources at terminals $k1$ and $k4$ are 0 and 20 degrees, respectively. The available measurements are the three phase instantaneous voltages and currents at two terminals of the line, with 5 ms data window and 100-kilo samples/sec sampling rate. Cubic spline interpolation method is adopted to complete the measurement set.

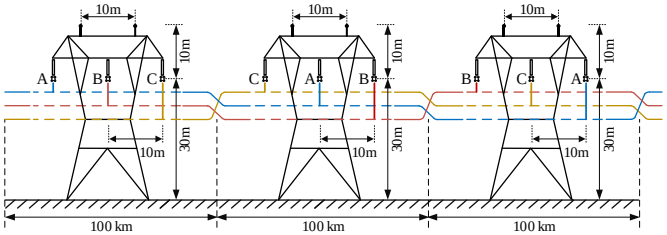

Figure. 4. Tower structure of the Practically transposed line

Here the proposed fault location method is compared to the existing voltage method which calculates the voltage distribution using the Bergeron model with ITLM. The calculation of the voltage distribution is also according to (7), but the practically transposed transmission line is assumed to be ideally transposed with homogeneous line parameters for entire transmission line (the line is transposed for infinite times to ensure absolute symmetry). For the existing method, the Clarke transformation is applied to decouple the system and the fault location algorithm is the same as in section III. The absolute fault location error in percentage is defined as the absolute error of fault location divided by the length of the entire transmission line.

Before the fault location test, the solution of the voltage distribution is firstly validated with pre-fault conditions. The line mode voltage distribution along entire practically transposed line solved from terminal $k1$ with the proposed method and the existing method is shown in Figure 5 (a). The red line shows the results calculated with the proposed PTLM, the black line shows the results with the existing ITLM. The solid line shows the results for voltage distribution with phase angle of 0 degree (the phase angle of phase A voltage for the source at terminal $k1$), the dot line shows the results for voltage distribution with phase angle of 90 degree (this voltage is reduced by 1000 kV to uniform the coordinate). The real voltage distribution should be the broken line due the practically transposition, which is exactly the solution with the proposed method. On the other hand, for the ITLM, the model is only equivalent to the PTLM at line terminals (as can be observed from the figure). With accurate solution of the voltage distribution, the proposed fault location method is expected to have less fault location error.

Next, five groups of faults with different fault types, fault impedances and fault locations are tested, including low impedance phase A to G faults, high impedance phase A to G faults, low impedance phase B to C faults, low impedance phase BC to G faults and three phase faults. For each fault type and fault impedance, the actual fault location is set as 2 km, 298 km and every 20 km from [20, 280] km from terminal $k1$.

A. Low Impedance Phase A to G Fault

The fault location results of low impedance phase A to G faults are shown in Figure 5 (b). The average absolute errors and maximum absolute errors of the proposed method and existing method are summarized in the first row of Table 1.

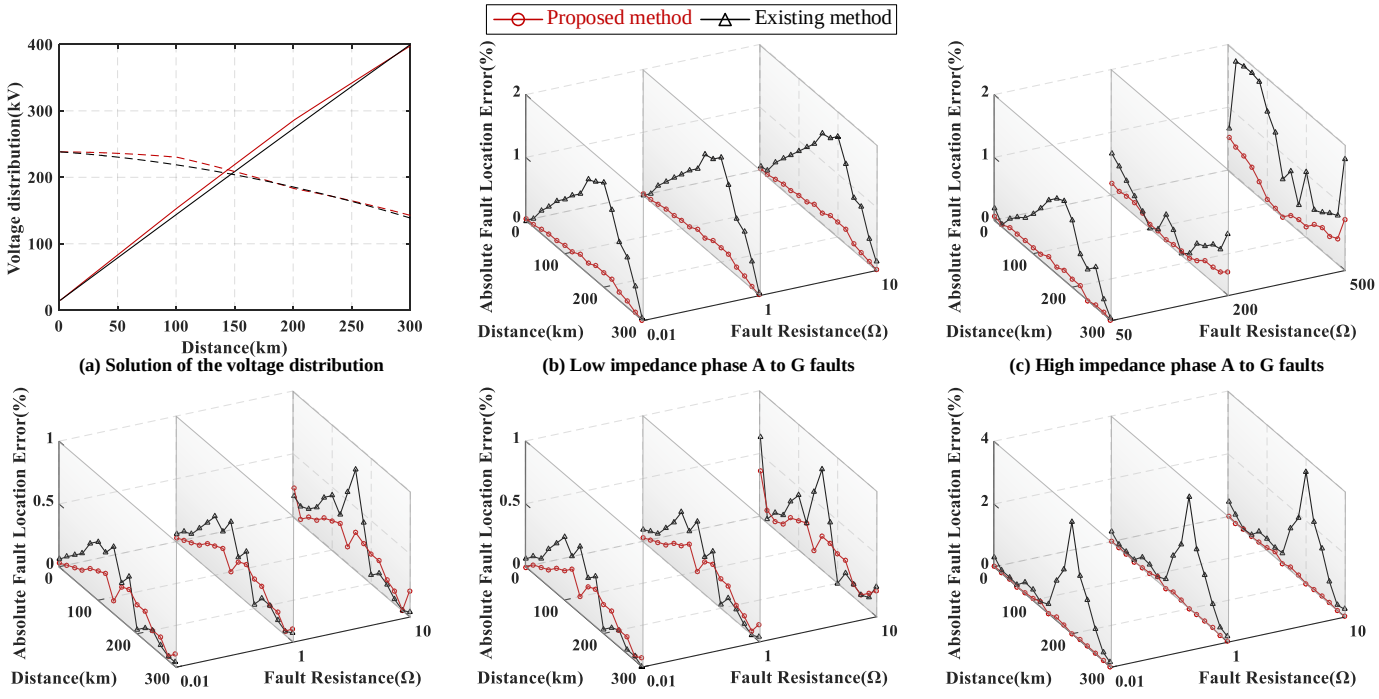

(a) Solution of the voltage distribution

(b) Low impedance phase A to G faults

(c) High impedance phase A to G faults

(d) Low impedance phase B to C faults

(e) Low impedance phase BC to G faults

(f) Low impedance Three phase faults

Figure. 5. Solution of the voltage distribution and absolute fault location error with different fault types, fault locations and fault impedances

Table. 1. Average absolute errors (%) and maximum absolute errors (%) for faults with different fault types and fault impedances

Fault type	Fault resistance	Average error (%)		Maximum error (%)	
		Proposed method	Existing method	Proposed method	Existing method
Low resistance A-G	0.01 (Ω)	0.12	0.82	0.23	1.67
	1 (Ω)	0.12	0.81	0.23	1.67
	10 (Ω)	0.12	0.79	0.23	1.60
High resistance A-G	50 (Ω)	0.09	0.59	0.17	1.27
	200 (Ω)	0.16	0.39	0.37	0.97
	500 (Ω)	0.30	1.13	0.80	1.87
B-C	0.01 (Ω)	0.16	0.23	0.30	0.53
	1 (Ω)	0.16	0.22	0.30	0.53
	10 (Ω)	0.18	0.25	0.30	0.80
BC-G	0.01 (Ω)	0.16	0.22	0.30	0.53
	1 (Ω)	0.16	0.22	0.30	0.53
	10 (Ω)	0.18	0.28	0.37	0.80
Three phase	0.01 (Ω)	0.04	0.83	0.17	3.57
	1 (Ω)	0.04	0.83	0.17	3.57
	10 (Ω)	0.04	0.86	0.17	3.57

B. High Impedance Phase A to G Fault

The fault location results of high impedance phase A to G faults are shown in Figure 5 (c). The average absolute errors and maximum absolute errors of the proposed method and existing method are summarized in the second row of Table 1.

C. Low Impedance Phase B to C Fault

The fault location results of low impedance phase B to C faults are shown in Figure 5 (d). The average absolute errors and maximum absolute errors of the proposed method and existing method are summarized in the third row of Table 1.

D. Low Impedance Phase BC to G Fault

The fault location results of low impedance phase BC to G faults are shown in Figure 5 (e). The average absolute errors and maximum absolute errors of the proposed method and existing method are summarized in the fourth row of Table 1.

E. Low Impedance Three Phase Fault

The fault location results of low impedance three phase faults are shown in Figure 5 (f). The average absolute errors and maximum absolute errors of the proposed method and existing method are summarized in the fifth row of Table 1.

F. Summary

To sum up, the fault location results with the proposed method present less error compared to the existing method that treats the practically transposed transmission line as ideally transposed transmission line. Note that for fault occurs close to the terminals of the transmission line, the fault location error of the existing method is comparable to the proposed method. This is exactly because only at terminals of the line, the ITLM is equivalent to the PTLM. For fault occurs in the middle of the line, the proposed method results in less fault location error, with more accurate modeling of the practically transposed transmission line.

V. CONCLUSION

This paper proposes a time domain fault location method for practically transposed transmission line. The practically transposed line that is transposed for limited times is modeled as a non-homogeneous line with several untransposed line sections. The matrix form partial differential equations describe the physical laws of the practical transmission line model with distributed parameters in time domain. The eigenvalue decomposition is applied to decouple the untransposed three phase line section into single mode lines and the Bergeron model is adopted to solve the single mode lines. Afterwards, the voltage distribution along entire practically transposed line is solved. With the detail modeling of the practically transposed line, the solutions of the voltage distribution of the proposed method is more accurate than those of the existing method. With the accurate solution of the voltage distributions, the voltage method is applied to solve the fault location. Extensive numerical experiments in a 300 km three phase practically transposed transmission line show that, the proposed fault location method have less fault location error compare to the existing fault location method that assumes ideal transposition, independent of fault types, fault impedances and fault locations, with 5 ms data window.

REFERENCES

[1] S. Das, S. Santoso, A. Gaikwad and M. Patel., "Impedance-based fault location in transmission networks: theory and application," *IEEE Access*, vol. 2, pp. 537– 557, Feb. 2014.

[2] C.Y. Evrenosoglu amd A. Abur, "Travelling wave based fault location for teed circuits," *IEEE Trans. Power Del*., vol. 20, no. 2, pp. 1115–1121, Apr. 2005.

[3] M. Gilany, D. k. Ibrahim and E. S. Tag Eldin, "Traveling-Wave-Based Fault-Location Scheme for Multiend-Aged Underground Cable System," *IEEE Trans. Power Del*., vol. 22, no. 1, pp. 82-89, Jan. 2007.

[4] F. V. Lopes, K. M. Dantas, K. M. Silva and F. B. Costa, "Accurate two-terminal transmission line fault location using traveling waves," *IEEE Trans. Power Del.*, vol. 33, no. 2, pp. 873-880, Apr. 2018.

[5] N. Kang, J. Chen and Y. Liao, "A Fault-Location algorithm for series-compensated double-circuit transmission lines using the distributed parameter line model," *IEEE Trans. Power Del*., vol. 30, no. 1, pp. 360-367, Feb. 2015.

[6] C. Chen, C. Liu and J. Jiang, "A new adaptive PMU based protection scheme for transposed/untransposed parallel transmission lines," *IEEE Trans. Power Del*., vol. 17, no. 2, pp. 395-404, April 2002.

[7] S. Kang, Y. Ahn, Y. Kang and S. Nam, "A Fault Location Algorithm Based on Circuit Analysis for Untransposed Parallel Transmission Lines," *IEEE Trans. Power Del*., vol. 24, no. 4, pp. 1850-1856, Oct. 2009.

[8] Y. Liu, B. Wang, X. Zheng, D. Lu, M. Fu and N. Tai, "Fault location algorithm for non-homogeneous transmission lines considering line asymmetry," *IEEE Trans. Power Del.*, 2020, early access.

[9] M. B. Djuric, Z. M. Radojevic, and V. V. Terzija. "Time domain solution of fault distance estimation and arcing faults detection on overhead lines," *IEEE Trans. Power Del*., vol 14, no. 1: pp. 60-67, Feb. 1999.

[10] Y. Liu, S. Meliopoulos, Z. Tan, L. Sun and R. Fan, "Dynamic state estimation-based fault locating on transmission lines," *IET Generation Transmission Distribution*, vol. 11, no. 17, pp. 4184-4192, Nov. 2017.

[11] R. Fan, Y. Liu, R. Huang, R. Diao and S. Wang, "Precise Fault Location on Transmission Lines Using Ensemble Kalman Filter," *IEEE Trans Power Del.*, vol. 33, no. 6, pp. 3252-3255, Dec. 2018.

[12] J. Suonan, S. Gao, G. Song, Z. Jiao and X. Kang, " A novel fault-location method for HVDC transmission lines," *IEEE Trans. Power Del.*, vol. 25, no. 2, pp. 1203-1209, Apr. 2010.

[13] D. Lu, Y. Liu, Q. Liao, B. Wang, W. Huang and X. Xi, "Time-domain transmission line fault location method with full consideration of distributed parameters and line asymmetry," *IEEE Trans. Power Del*., early access.

[14] C. E. M. Pereira and L. C. Zanetta, "Optimization algorithm for fault location in transmission lines considering current transformers saturation," *IEEE Trans. Power Del.*, vol. 20, no. 2, pp. 603-608, April 2005.

[15] R. Schulze and P. Schegner, "A new fault location method for transmission lines taking the places of transposing into account," *IEEE Power Energy Soc. Gen. Meet.*, Detroit, MI, USA, 2011.

[16] D. Lu, Y. Liu, W. Huang and X. Xi, "Accurate fault location in AC/DC hybrid line corridors based on eigenvalue decomposition," *IEEE Power Energy Soc. Gen. Meet.*, Montreal, PQ, CAN, 2020.

[17] H. W. Dommel, "Digital computer solution of electromagnetic transients in single- and multiphase networks," *IEEE Transactions on Power Apparatus and Systems*, vol. PAS-88, no. 4, pp. 388–399, April 1969.